



**HAL**  
open science

## ITRF2020 Plate Motion Model

Zuheir Altamimi, L. Métivier, Paul Rebischung, Xavier Collilieux, Kristel Chanard, Julien Barnéoud

► **To cite this version:**

Zuheir Altamimi, L. Métivier, Paul Rebischung, Xavier Collilieux, Kristel Chanard, et al.. ITRF2020 Plate Motion Model. *Geophysical Research Letters*, 2023, 50 (24), 10.1029/2023GL106373. hal-04371259

**HAL Id: hal-04371259**

**<https://hal.science/hal-04371259>**

Submitted on 4 Jan 2024

**HAL** is a multi-disciplinary open access archive for the deposit and dissemination of scientific research documents, whether they are published or not. The documents may come from teaching and research institutions in France or abroad, or from public or private research centers.

L'archive ouverte pluridisciplinaire **HAL**, est destinée au dépôt et à la diffusion de documents scientifiques de niveau recherche, publiés ou non, émanant des établissements d'enseignement et de recherche français ou étrangers, des laboratoires publics ou privés.



Distributed under a Creative Commons Attribution - NonCommercial - ShareAlike 4.0 International License




# Geophysical Research Letters®



## RESEARCH LETTER

10.1029/2023GL106373

## ITRF2020 Plate Motion Model

Z. Altamimi<sup>1,2</sup> , L. Métivier<sup>1,2</sup> , P. Rebischung<sup>1,2</sup>, X. Collilieux<sup>1,2</sup>, K. Chanard<sup>1,2</sup>, and J. Barnéoud<sup>1,2</sup> 

<sup>1</sup>Université Paris Cité, Institut de Physique du Globe de Paris, CNRS, IGN, Paris, France, <sup>2</sup>University Gustave Eiffel, ENSG, IGN, Marne-la-Vallée, France

### Key Points:

- We derive a plate motion model for 13 tectonic plates from the ITRF2020 horizontal velocity field
- Built under the rigid-plate motion hypothesis, the model represents the ITRF2020 velocity field with a precision of 0.25 mm/yr WRMS
- The residual velocities would show a global northward motion if a translation rate was not included in the inversion model

### Supporting Information:

Supporting Information may be found in the online version of this article.

### Correspondence to:

Z. Altamimi,  
[zuheir.altamimi@ign.fr](mailto:zuheir.altamimi@ign.fr)

### Citation:

Altamimi, Z., Métivier, L., Rebischung, P., Collilieux, X., Chanard, K., & Barnéoud, J. (2023). ITRF2020 plate motion model. *Geophysical Research Letters*, 50, e2023GL106373. <https://doi.org/10.1029/2023GL106373>

Received 13 SEP 2023  
Accepted 19 NOV 2023

### Author Contributions:

**Conceptualization:** Z. Altamimi  
**Formal analysis:** Z. Altamimi, L. Métivier, P. Rebischung, X. Collilieux, K. Chanard, J. Barnéoud  
**Investigation:** L. Métivier, P. Rebischung, X. Collilieux, K. Chanard, J. Barnéoud  
**Methodology:** Z. Altamimi, L. Métivier  
**Software:** Z. Altamimi  
**Supervision:** Z. Altamimi  
**Visualization:** Z. Altamimi  
**Writing – original draft:** Z. Altamimi

**Abstract** A tectonic Plate Motion Model (PMM) is essential for geodetic applications, while contributing to the understanding of geodynamic processes affecting the Earth's surface. We introduce a PMM derived from the horizontal velocities of 518 sites extracted from the ITRF2020 solution. These sites were chosen away from plate boundaries, Glacial Isostatic Adjustment regions, and other deforming zones. Unlike the ITRF2014-PMM, which showed no significant Origin Rate Bias (ORB), velocities used to determine the ITRF2020-PMM exhibit a statistically significant ORB ( $0.74 \pm 0.09$  mm/yr along the Z-component). Users are advised to add the estimated ORB to the horizontal velocities predicted by the ITRF2020-PMM rotation poles for full consistency with the ITRF2020. However, the predicted vertical velocities resulting from the addition of the ORB should be discarded. The overall precision with which the ITRF2020 velocity field is represented by the rigid ITRF2020-PMM is at the level of 0.25 mm/yr WRMS.

**Plain Language Summary** The Earth's surface is divided in large and small tectonic plates, which evolve and move slowly over time, resulting in lateral displacements of the ground surface typically of the order of a few cm/yr. Because of the relative motion between tectonic plates, plate boundaries can be either divergent (when two plates move away from each other), convergent (when two plates collide) or transform (when two plates slide past each other). Plate motion models are used to quantify the relative motions of the plates with respect to each other, and are determined using geological data or observations collected by space geodesy instruments distributed over different plates at the Earth's surface. In the latter case, space geodesy observations from the four space geodetic techniques covering more than 40 years of data are analyzed to estimate the long-term displacements (or velocities) of each instrument in a well defined and self-consistent global reference frame. The derived velocity field is then used to estimate a comprehensive plate motion model (PMM). This article presents a PMM for 13 tectonic plates based on a subset of the velocity field from the recently released International Terrestrial Reference Frame 2020 (ITRF2020); see <https://itrf.ign.fr/en/solutions/ITRF2020>.

## 1. Introduction

Global Plate Motion Models (PMMs) play a crucial role in describing and understanding the continuously deforming Earth's surface, especially the geological processes occurring at plate boundaries and their relationship with seismicity and volcanic activity. While early PMM were determined using geological and geophysical data (DeMets et al., 1994, 2010; Minster & Jordan, 1978), modern space-geodesy-based absolute PMM are determined using velocity fields from long-term observations of geodetic stations. Previous publications, such as Altamimi et al. (2012, 2017), provide a representative list of geological and space-geodesy-based models.

Together with a reference frame, such as the International Terrestrial Reference Frame (ITRF), global PMM are also needed for positioning applications at the Earth's surface, or for defining some continental reference frames (Altamimi & Boucher, 2002; Blewitt et al., 2013; Herring et al., 2016).

The velocity field obtained from the latest release of the ITRF (ITRF2020; Altamimi et al., 2023) benefits from an improved data analysis strategy, where nonlinear station motions are accurately modeled, including annual and semi-annual signals and post-seismic displacements for sites affected by major earthquakes. By estimating annual and semi-annual signals, we have demonstrated a reduction of about 10% in formal errors of station velocities, indicating an improved determination of the ITRF2020 velocity field. Furthermore, as the successive ITRF solutions include more and more sites with longer and longer observation spans, their associated PMM improve over time. Therefore, the ITRF2020-PMM introduced in this study is expected to be more accurate than its previous versions since it includes about 6 years of additional data. Moreover, ITRF2020-PMM is intended to serve operational geodetic applications such as the definition of regional reference frames consistent with

© 2023. The Authors.

This is an open access article under the terms of the [Creative Commons Attribution-NonCommercial-NoDerivs License](https://creativecommons.org/licenses/by-nc-nd/4.0/), which permits use and distribution in any medium, provided the original work is properly cited, the use is non-commercial and no modifications or adaptations are made.

ITRF2020 and the prediction of ITRF2020-compatible horizontal velocities in areas not covered by the ITRF network.

In this study, we first provide in Section 2 a brief description of our inversion models for estimating PMM from a global velocity field. In Section 3, we describe the criteria used for the selection of a subset of ITRF2020 sites on which the ITRF2020-PMM is based. Section 4 details the data analysis process, while Section 5 presents the ITRF2020-PMM and its recommended usage. Finally, in Section 6, we discuss the comparison between the new ITRF2020-PMM and its predecessor, the ITRF2014-PMM (Altamimi et al., 2017).

## 2. Inversion Models

While past publications introduced two possible PMM inversion models (e.g., Altamimi et al., 2017), they are presented here again for completeness and to contextualize the discussion of this paper.

To estimate the rotation pole  $\omega_p$  (or angular velocity) of a given plate  $p$ , based on the horizontal velocities of a set of points on that plate, the classical inversion model takes the form:

$$\dot{X}_i = \omega_p \times X_i \quad (1)$$

Here  $\dot{X}_i$  and  $X_i$  represent the velocity and the position vectors of point  $i$ , respectively. Note that the vertical component of vector  $\dot{X}_i$  is set to zero, ensuring that vertical velocities do not interfere in PMM estimation.

In the following sections, we explain and justify reasons that led us to use an alternative inversion model. This model includes an unknown translation rate  $\dot{T}$ , called here an Origin Rate Bias (ORB), a concept previously investigated by Argus (2007), Kogan and Steblov (2008), and Altamimi et al. (2012):

$$\dot{X}_i = \omega_p \times X_i + \dot{T} \quad (2)$$

Note that estimating an ORB can be meaningful only when multiple plate rotation poles are determined simultaneously.

According to Blewitt (2003), the ORB  $\dot{T}$  in Equation 2 theoretically represents the translation rate between the Earth's Center of Mass (CM, the theoretical origin of the ITRF velocities) and a “residual” center of surface lateral figure (the origin with respect to which the surface integral of horizontal velocities corrected from the estimated PMM is zero). However, in practice, the selected sites are far from providing a uniform discretization of all tectonic plates. Additionally, the ORB estimation strongly relies on the specific selection of sites used in the inversion (see detailed discussion in Altamimi et al. (2017)). It is therefore hazardous to attribute any actual geophysical meaning to the estimated ORB.

## 3. Site Selection

We refined the criteria for site selection operated in the determination of the ITRF2014-PMM (Altamimi et al., 2017). For the ITRF2020-PMM inversion, the sites selected meet the following enhanced conditions: (a) the time span of observations per site is longer than three years, (b) the sites are at least 100 km away from Bird (2003)'s plate boundaries and outside areas that show significant intraplate tectonic deformation (as defined below), (c) far from Glacial Isostatic Adjustment (GIA) regions (as defined below), (d) outside regions impacted by present-day ice melting or by significant trends in continental hydrology (as defined below), and (e) normalized post-fit velocity residuals (raw residuals divided by their a priori uncertainties and the posteriori variance factor) remain under 3, and raw residuals are below 1 mm/yr.

As in Altamimi et al. (2017), we have identified regions with significant “intraplate tectonic deformation” from the global strain rate map published by Kreemer et al. (2014). However, while we chose to exclude all sites in regions that had strain rates to obtain ITRF2014-PMM (Altamimi et al., 2017), even those close to zero, here we opted for a more refined approach. We defined the tectonic regions from their strain rate values and excluded all sites located in regions where the second invariant of the strain rate tensor was larger than  $4 \times 10^{-9} \text{ yr}^{-1}$ . We estimated that local deformation can be considered as negligible below this value. As proposed by Altamimi et al. (2017), we define “GIA regions” as areas which are expected to show large GIA induced vertical velocities. We adopted ICE-6G GIA model (Peltier et al., 2015) to identify sites with predicted vertical velocities larger than

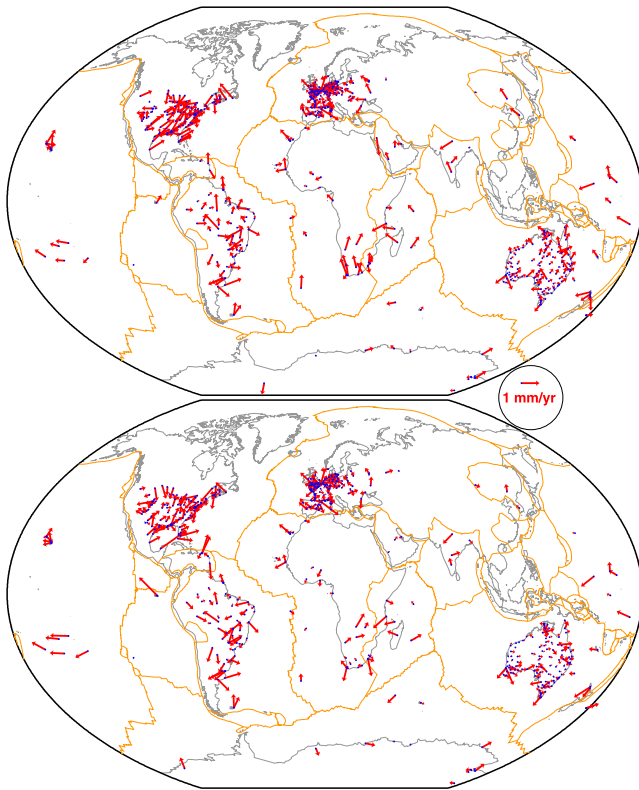


**Figure 1.** Post-fit residuals without (top, involving 510 sites) and with (bottom, involving 518 sites) Origin Rate Bias included in the inversion model. Plate boundaries from Bird (2003) are shown in orange.

0.8 mm/yr. A few stations located in Scandinavia, Faroe Islands or Shetland islands, which do not meet the criterion, have also been discarded due to their evident proximity to GIA regions. We do not consider GIA horizontal velocity predictions in our selection, given the results of Altamimi et al. (2012) that are still valid today. Indeed, we observe large differences in horizontal velocity predictions between the few existing GIA models. In Altamimi et al. (2012), we showed that correcting horizontal velocities with GIA predictions did not improve the fit. Here we additionally tested the ICE-6G GIA model (Peltier et al., 2015), which is more recent than those previously evaluated. Although more realistic in some respects than the previous ones, this model unfortunately does not reduce the residuals associated with the plate model calculations. The overall WRMS values have indeed increased by 20% and 30% in East and North components, respectively. As a reminder, Altamimi et al. (2017) showed that GIA may induce horizontal velocities far from the so-called GIA regions at a level up to 3–4 mm/yr. As a consequence, ITRF2020-PMM, as all past geodetic PMM, may be slightly but significantly contaminated by GIA. Finally, present-day ice melting regions or the areas impacted by significant hydrological signals have been defined as the regions where the surface loads taken from Gauer et al. (2023)'s GRACE and GRACE-FO solutions induce horizontal velocities larger than 0.23 mm/yr over the period 2003–2021 (in a frame centered on the center of surface lateral figure as defined by Blewitt (2003)). This criterion has been empirically chosen in order to exclude stations with evident non-tectonic plate motions. This concerns only a few stations subject to ice melting in Greenland, Antarctica and Alaska. The impact of recent hydrological trends, although far from negligible on local vertical velocities, appears very small, for now, on horizontal velocities. Note that most of stations located in Greenland and in the Antarctica Peninsula have been excluded whether or not they met the criterion, due to local clear evidences of ice melting impact (e.g., if the station shows a very large vertical velocity).

Finally, like for the ITRF2014-PMM, we did not exclude sites located in Antarctica (except in the Antarctica Peninsula) from our selection in order to provide a rotation pole for that plate, and because tests described in Altamimi et al. (2017) showed that GIA would bias the estimated Antarctica rotation pole only marginally.

We found in total 647 sites satisfying the four first conditions, including the retained Antarctica sites, whose horizontal velocities were extracted from the ITRF2020 global solution (Altamimi et al., 2023), with full variance-covariance information.

#### 4. Data Analysis

Starting with the set of 647 sites, we implement an iterative inversion based on the model described in Equation 1, without ORB. Throughout this process, we progressively reject sites that failed to satisfy condition (e). The iterative inversion resulted in 510 sites spanning over 13 tectonic plates. Note that, similar to our procedure used in the ITRF2014-PMM inversion, we re-specified the reference frame effect of the origin, scale and orientation of the selected velocity field, at the level of 0.1 mm/yr. This was achieved using the so-called inner constraints approach (Sillard & Boucher, 2001), by modifying its variance-covariance matrix, using Equation A15 of Altamimi et al. (2002)—without however modifying the values of the velocities. Failing to do so would introduce systematic velocity residuals due to the network effect.

Figure 1 (top panel) illustrates the distribution and post-fit velocity residuals of the 510 selected sites. Although the site velocity residuals meet condition (e), with normalized residuals below 3 and raw residuals under 1 mm/yr, a subtle systematic northward residual motion can be observed. This residual motion is particularly clear in regions like Australia, North America, the northern part of South America, western Pacific and southern Africa. The WRMS values of the East and North velocity residuals are 0.23 and 0.27 mm/yr, respectively.

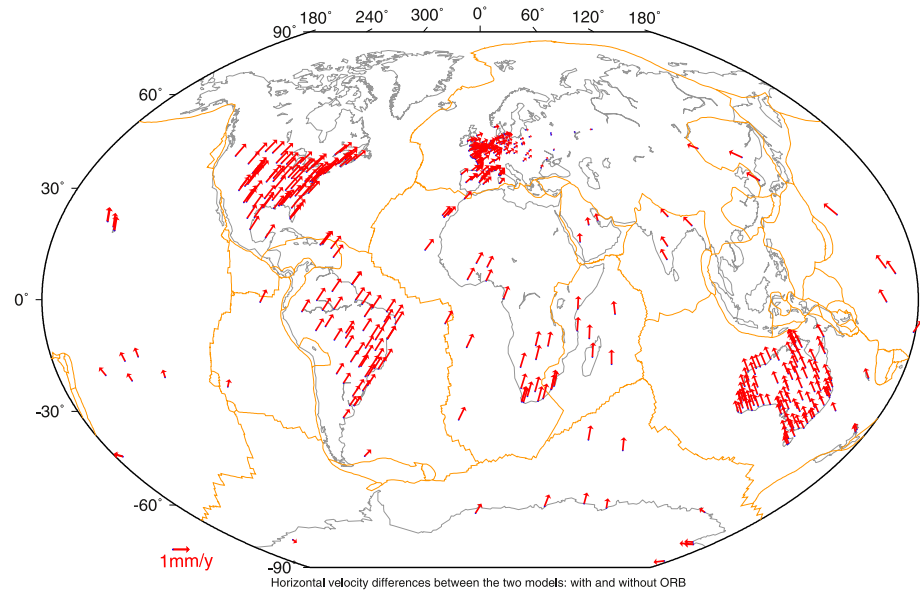


**Figure 2.** Horizontal velocity differences between the two models: with minus without Origin Rate Bias estimated.

The observed pattern, combined with the need to account for a potential ORB in the selected velocity field, led us to employ an iterative inversion based on the model given by Equation 2. The second iterative inversion resulted in a final site selection containing 518 points. The three components of the estimated ORB emerged as statistically significant:  $0.37 \pm 0.08$ ,  $0.35 \pm 0.10$ , and  $0.74 \pm 0.09$  mm/yr for  $\dot{T}_X$ ,  $\dot{T}_Y$ , and  $\dot{T}_Z$ , respectively. By including the ORB into the inversion model, the systematic northward residual motion was largely mitigated (as seen when comparing top and bottom panels of Figure 1). The WRMS of the velocity residuals were also reduced to 0.21 and 0.24 mm/yr for the East and North components, respectively. The velocity differences between the two models (with minus without ORB estimated) are illustrated in Figure 2. While the ITRF2014-PMM inversion (Altamimi et al., 2017) did not reveal a statistically significant ORB, it appears necessary to include an ORB in the ITRF2020-PMM inversion. We recall that the ORB of ITRF2014-PMM was statistically not far from zero at the 2-sigma level:  $0.20(\pm 0.15)$ ,  $0.00(\pm 0.18)$ , and  $0.30(\pm 0.18)$  mm/yr, for  $\dot{T}_X$ ,  $\dot{T}_Y$ , and  $\dot{T}_Z$ , respectively. The  $\pm$  figures between parentheses are 1-sigma values.

## 5. ITRF2020 Plate Motion Model and Its Usage

Based on the analysis presented in the previous section, the ITRF2020-PMM is made up of plate rotation poles plus a 3-dimensional translation rate. Table 1 lists the ITRF2020 absolute rotation poles of the 13 plates, while Table 2 lists the three components of the associated ORB. Furthermore, Table 1 also provides the WRMS of the adjustment residuals for each one of the 13 plates, as well as the overall WRMS of the ITRF2020-PMM adjustment residuals, which are about 0.25 mm/yr.

In order to be consistent with the ITRF2020 frame, users of the ITRF2020-PMM should not only use the plate rotation poles listed in Table 1, but also add the translation rates listed in Table 2. However, it is recommended to ignore the artifactual vertical component of the predicted velocities resulting from the addition of the ORB, and to only consider the horizontal components of the predicted velocities.

Caution should be observed when using rotation poles of plates with large uncertainties, since they were determined from a small number of sites, such as the Amurian, Arabian, Caribbean, Indian, and Nazca plates.

We provide in Supporting Information S1 the following tables:

- Table S1 in Supporting Information S1: ITRF2020-PMM plate rotation poles and ORB components in a machine-readable file;
- Table S2 in Supporting Information S1: list of the 518 selected sites and their ITRF2020 horizontal velocities, together with their formal errors and post-fit residuals.



**Table 1**  
*Absolute Plate Rotation Poles Defining the ITRF2020-Plate Motion Model and Their Standard Deviations (1-Sigma)*

Plate	NS <sup>a</sup>	$\omega_x$	$\omega_y$	$\omega_z$	$\omega$	WRMS	
						E	N
			mas/yr		°/Ma	mm/yr	
AMUR	3	-0.131	-0.551	0.837	0.281	0.17	0.18
±		0.009	0.014	0.015	0.002		
ANTA	15	-0.269	-0.312	0.678	0.220	0.16	0.24
±		0.003	0.003	0.004	0.001		
ARAB	3	1.129	-0.146	1.438	0.509	0.15	0.11
±		0.025	0.027	0.016	0.007		
AUST	118	1.487	1.175	1.223	0.627	0.19	0.17
±		0.003	0.003	0.003	0.001		
CARB	5	0.207	-1.422	0.726	0.447	0.18	0.56
±		0.076	0.174	0.061	0.053		
EURA	143	-0.085	-0.519	0.753	0.255	0.19	0.21
±		0.003	0.003	0.003	0.001		
INDI	4	1.137	0.013	1.444	0.511	0.41	0.33
±		0.008	0.040	0.016	0.005		
NAZC	3	-0.327	-1.561	1.605	0.629	0.05	0.10
±		0.006	0.018	0.008	0.003		
NOAM	108	0.045	-0.666	-0.098	0.187	0.23	0.31
±		0.003	0.003	0.003	0.001		
NUBI	31	0.090	-0.585	0.717	0.258	0.18	0.21
±		0.003	0.003	0.004	0.001		
PCFC	20	-0.404	1.021	-2.154	0.672	0.32	0.30
±		0.003	0.003	0.004	0.001		
SOAM	59	-0.261	-0.282	-0.157	0.115	0.30	0.29
±		0.004	0.004	0.003	0.001		
SOMA	6	-0.081	-0.719	0.864	0.313	0.41	0.21
±		0.014	0.015	0.005	0.004		
ITRF2020-PMM overall fit						0.21	0.24

<sup>a</sup>Number of sites.

**Table 2**  
*Components of the Origin Rate Bias of the ITRF2020-Plate Motion Model and Their Standard Deviations (1-Sigma)*

$\dot{T}_x$	$\dot{T}_y$	$\dot{T}_z$
mm/yr		
0.37	0.35	0.74
±0.08	±0.10	±0.09

## 6. Comparison With the ITRF2014-PMM

Comparisons between the ITRF2014-PMM and the ITRF2008-PMM, as well as with two geological models: NNR-NUVEL-1A (Argus & Gordon, 1991) and NNR-MORVEL56 (Argus et al., 2011), were discussed in Altamimi et al. (2012) and in Altamimi et al. (2017), and are not worth repeating here.

The differences between the site velocities predicted by the two models ITRF2020-PMM and ITRF2014-PMM (that has no ORB) are provided in Figure 3. They show rotational-type differences for specific plates, but more complex patterns for others like the Nubia or Pacific plates, likely due to the impact of the ORB.

While differences in the predicted velocity differences plotted in Figure 3 show plate-specific patterns, we estimated three global rotation rates between the two predicted velocity fields and found the following values (from ITRF2020-PMM to ITRF2014-PMM): +3, -4, and +4 micro-arc-seconds per year around the X, Y, and Z axes, respectively. These values are negligible, as expected, due to the successive alignment of the ITRF solutions in orientation time evolution. The WRMS of residuals, about 0.1 mm/yr, is an indication of the overall precision of the ITRF plate motion models, at least for plates with large number of sites.

## 7. Conclusion

Following the series of ITRF plate motion models, this paper describes the main features of the ITRF2020-PMM which is made up of rotation poles for 13 tectonic plates plus a 3-dimensional translation rate (ORB). The selected field of 518 ITRF2020 horizontal velocities indeed exhibits a statistically significant ORB (up to  $0.74 \pm 0.09$  mm/yr along the Z component). It remains however hazardous to attribute any geophysical meaning to the estimated ORB. The overall precision with which the ITRF2020 velocity field is represented by the rigid ITRF2020-PMM is at the level of 0.25 mm/yr WRMS.

Users of the ITRF2020-PMM should use both the plate rotation poles and the ORB, so that the predicted velocities are fully consistent with the ITRF2020 frame. However, the artifactual vertical component of the predicted velocities resulting from the addition of the ORB should be discarded.

Although the 518 selected sites are strategically chosen away from GIA regions, except in Antarctica, GIA could still influence the estimated rotation poles of specific plates (particularly the North American plate). Therefore, it is not recommended to subtract the ITRF2020-PMM from observed velocities in order to isolate GIA deformation.

Considering that the successive ITRF solutions are all aligned to each other in orientation time evolution, and that the accuracy of the time evolution of the ITRF long-term origin is at the level of 0.5 mm/yr (Altamimi et al., 2023), the past ITRF-PMM dating back to ITRF2005 can be considered nearly equivalent to each other at the level of 0.5 mm/yr. We believe however that the ITRF2020-PMM is more robust and more accurate than its predecessors, as more sites with longer data spans were used in its elaboration.

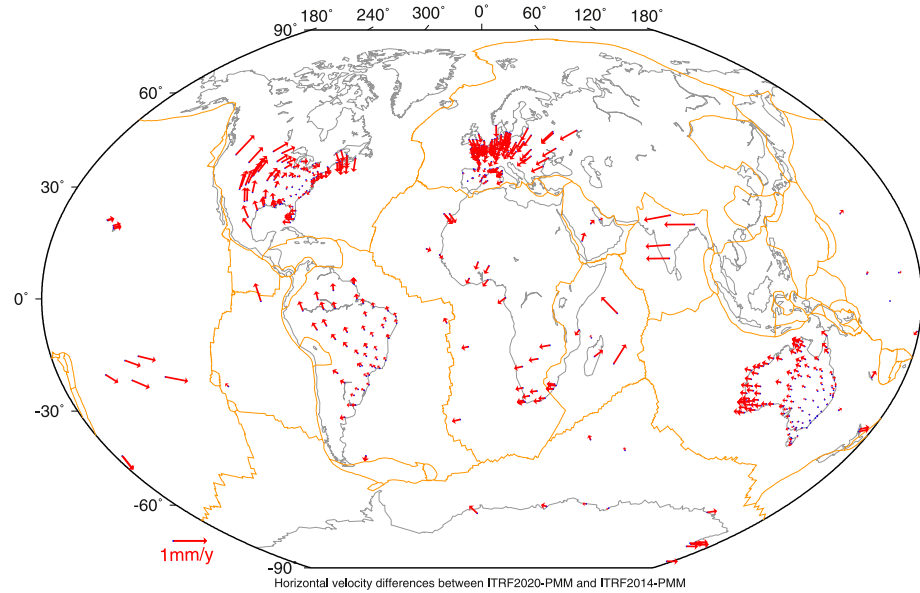


**Figure 3.** Differences between horizontal velocities predicted by ITRF2020-PMM and the ITRF2014-PMM (ITRF2020-PMM minus ITRF2014-PMM).

## Data Availability Statement

All the data used in this study is available at the ITRF2020 web site. Please see Altamimi et al. (2022).

## Acknowledgments

The International Terrestrial Reference Frame (ITRF) is the result of a global collaboration of hundreds of institutions around the world: from the build-up of geodetic observatories, satellite missions, data collection, analysis, and combination, to the ITRF generation, thanks to the investment of national mapping agencies, space agencies, universities, and research institutes. The ITRF activities are funded by the Institut national de l'information géographique et forestière (IGN), France, and partly by Centre National d'Etudes Spatiales (CNES). This study contributes to the IdEx Université de Paris ANR-18-IDEX-0001. We thank Corné Kreemer for providing his global strain map. We acknowledge helpful comments and suggestions provided by two anonymous reviewers which improved the content of this article.

## References

- Altamimi, Z., & Boucher, C. (2002). The ITRS and ETRS89 relationship: New results from ITRF2000. In *Proceedings of the EUREF symposium, Dubrovnik, 16-18 May 2001*. Verlag des Bundesamts für Kartographie und Geodäsie.
- Altamimi, Z., Métivier, L., & Collilieux, X. (2012). ITRF2008 plate motion model. *Journal of Geophysical Research*, *117*(B7), B07402. <https://doi.org/10.1029/2011JB008930>
- Altamimi, Z., Métivier, L., Rebischung, P., Rouby, H., & Collilieux, X. (2017). ITRF2014 plate motion model. *Geophysical Journal International*, *209*(3), 1906–1912. <https://doi.org/10.1093/gji/ggx136>
- Altamimi, Z., Rebischung, P., Collilieux, X., Métivier, L., & Chanard, K. (2022). ITRF2020 [Dataset]. IERS ITRS Center Hosted by IGN and IGP. Retrieved from <https://itrf.ign.fr/en/solutions/ITRF2020>
- Altamimi, Z., Rebischung, P., Collilieux, X., Métivier, L., & Chanard, K. (2023). ITRF2020: An augmented reference frame refining the modeling of nonlinear station motions. *Journal of Geodynamics*, *97*(47), 47. <https://doi.org/10.1007/s00190-023-01738-w>
- Altamimi, Z., Sillard, P., & Boucher, C. (2002). ITRF2000: A new release of the international terrestrial reference frame for Earth science applications. *Journal of Geophysical Research*, *107*(B10), 2214. <https://doi.org/10.1029/2001JB000561>
- Argus, D. F. (2007). Defining the translational velocity of the reference frame of Earth. *Geophysical Journal International*, *169*(3), 830–838. <https://doi.org/10.1111/j.1365-246X.2007.03344.x>
- Argus, D. F., & Gordon, R. G. (1991). No-net-rotation model of current plate velocities incorporating plate motion model Nuvel-1. *Geophysical Research Letters*, *18*(11), 2038–2042. <https://doi.org/10.1029/91gl01532>
- Argus, D. F., Gordon, R. G., & DeMets, C. (2011). Geologically current motion of 56 plate relative to the no-net-rotation reference frame. *Geochemistry, Geophysics, Geosystems*, *12*(11), Q11001. <https://doi.org/10.1029/2011GC003751>
- Bird, P. (2003). An updated digital model of plate boundaries. *Geochemistry, Geophysics, Geosystems*, *4*(3), 1027. <https://doi.org/10.1029/2001GC000252>
- Blewitt, G. (2003). Self-consistency in reference frames, geocenter definition, and surface loading of the solid Earth. *Journal of Geophysical Research*, *108*(B2), 2103. <https://doi.org/10.1029/2002JB002082>
- Blewitt, G., Kreemer, C., Hammond, W., & Goldfarb, J. M. (2013). Terrestrial reference frame NA12 for crustal deformation studies in North America. *Journal of Geodynamics*, *72*, 11–24. <https://doi.org/10.1016/j.jog.2013.08.004>
- DeMets, C., Gordon, R. G., & Argus, D. F. (2010). Geologically current plate motions. *Geophysical Journal International*, *181*(1), 1–80. <https://doi.org/10.1111/j.1365-246X.2009.04491.x>
- DeMets, C., Gordon, R. G., Argus, D. F., & Stein, S. (1994). Effect of recent revisions of the geomagnetic reversal timescale on estimates of current plate motions. *Geophysical Research Letters*, *21*(20), 2191–2194. <https://doi.org/10.1029/94gl02118>
- Gauer, L.-M., Chanard, K., & Fleitout, L. (2023). Data-driven gap filling and spatio-temporal filtering of the GRACE and GRACE-FO records. *Journal of Geophysical Research: Solid Earth*, *128*(5), e2022JB025561. <https://doi.org/10.1029/2022JB025561>
- Herring, T. A., Melbourne, T. I., Murray, M. H., Floyd, M. A., Széluga, W. M., King, R. W., et al. (2016). Plate boundary observatory and related networks: GPS data analysis methods and geodetic products. *Reviews of Geophysics*, *54*(4), 759–808. <https://doi.org/10.1002/2016RG000529>
- Kogan, M. G., & Steblo, G. M. (2008). Current global plate kinematics from GPS (1995–2007) with the plate-consistent reference frame. *Journal of Geophysical Research*, *113*(B12), 4416. <https://doi.org/10.1029/2007JB005353>

- Kreemer, C., Blewitt, G., & Klein, E. C. (2014). A geodetic plate motion and global strain rate model. *Geochemistry, Geophysics, Geosystems*, 15(10), 3849–3889. <https://doi.org/10.1002/2014GC005407>
- Minster, J. B., & Jordan, T. H. (1978). Present-day plate motions. *Journal of Geophysical Research*, 83(B11), 5331–5354. <https://doi.org/10.1029/jb083ib11p05331>
- Peltier, W. R., Argus, D. F., & Drummond, R. (2015). Space geodesy constrains ice age terminal deglaciation: The global ICE-6G\_C (VM5a) model. *Journal of Geophysical Research: Solid Earth*, 120(1), 450–487. <https://doi.org/10.1002/2014JB011176>
- Sillard, P., & Boucher, C. (2001). Review of algebraic constraints in terrestrial reference frame datum definition. *Journal of Geodynamics*, 75(2–3), 63–73. <https://doi.org/10.1007/s001900100166>